Synthesis of MCM-41 with a Phosphonium Template

Debbie Baute,[†] Herbert Zimmermann,[‡] Shifi Kababya,[†] Shimon Vega,[†] and Daniella Goldfarb*,[†]

Chemical Physics Department, Weizmann Institute of Science, Rehovot 76100, Israel, and Max-Planck Institute for Medical Research, Heidelberg 69120, Germany

Received December 2, 2004. Revised Manuscript Received March 31, 2005

Cetyltrimethyl phosphonium bromide was successfully used as a template in the synthesis of MCM-41. The material was characterized by small-angle X-ray diffraction, transmission electron microscopy, nitrogen adsorption, and ^{29}Si, ^{13}C, and ^{31}P solid-state NMR spectroscopy. These results were compared with those of MCM-41 prepared with the conventional cetyltrimethylammonium bromide surfactant showing that the material is highly ordered. Interestingly, the materials showed a "temporary" hydrothermal stability induced by residual P_2O_5 produced by the calcination. NMR measurements on the reaction mixture showed that ^{31}P can be used as an excellent probe for in situ investigation of the formation mechanism.

Introduction

An extensive amount of work has been performed on ordered mesoporous materials, ever since their discovery in 1992.[1] These studies focused on synthesizing new materials using a variety of templates, searching for new applications, and exploring the various reaction mechanisms.[2−9] In general, templated mesoporous materials are formed through the condensation of inorganic precursors, most often silicates, around self-assembled structures of surfactant molecules in solution. Mesoporous materials with large surface areas and narrow pore size distributions are generated by removal of the encapsulated organic templates through calcination or extraction. One of the first and most-studied mesoporous materials is MCM-41, which has a hexagonal arrangement of pores and is synthesized with positively charged surfactants as templates. The most commonly used surfactants in the synthesis of MCM-41 have an ammonium headgroup like the alkyltri(m)ethylammonium halides, C_nTAX, where $n = 8, 10, ..., 22$ and X = Cl, Br.[10−12] Other, less popular, ammonium-based templates are lecithins,[13] gemini surfactants,[14] 1-alkyl-3-methylimidazolium salts,[15] and cetylpyridinium bromide.[16,17] While the special properties of MCM-41 are attractive for many applications, their realizations, however, are hampered by the relatively low hydrothermal stability of these mesoporous materials. The ways to improve the hydrothermal stability have been recently reviewed[6,18] and include the addition of salts,[19] pH adjustment during the synthesis,[20−25] and postsynthetic hydrothermal restructuring in water.[25] These treatments, however, complicate and lengthen the synthetic procedure. More recently, addition of zeolite nanocrystals to reaction gels was found to significantly improve the hydrothermal stability of Al−MCM-41.[18]

So far, there have been no reports of the use of phosphonium surfactants in the synthesis of mesoporous materials via the S^+I^- route,[26] although phosphate-based, negatively charged surfactants were used in the S^-I^+ pathway.[27] Phosphonium surfactants are sometimes mentioned in patents,[28] since their behavior in aqueous solution is very similar to that of the ammonium surfactants, but no descriptions were

* Corresponding author. E-mail: daniella.goldfarb@weizmann.ac.il. Phone: +972-8-9342016. Fax: +972-8-9344123.

[†] Weizmann Institute of Science.

[‡] Max-Planck Institute for Medical Research.

(1) Kresge, C. T.; Leonowicz, M. E.; Roth, W. J.; Vartuli, J. C.; Beck, J. S. *Nature* **1992**, *359*, 710.
(2) Ying, J. Y.; Mehnert, C. P.; Wong, M. S. *Angew. Chem., Int. Ed. Engl.* **1999**, *38*, 56.
(3) Patarin, J.; Lebeau, B.; Zana, R. *Curr. Opin. Coll. Interface Sci.* **2002**, *7*, 107.
(4) Stein, A. *Adv. Mater.* **2003**, *15*, 763.
(5) Zhao, D. *Curr. Opin. Solid State Mater. Sci.* **2003**, *7*, 191.
(6) Linssen, T.; Cassiers, K.; Cool, P.; Vansant, E. F. *Adv. Coll. Inter. Sci.* **2003**, *103*, 121.
(7) Davis, M. E. *Nature* **2002**, *417*, 813.
(8) Soler-Illia, D. J. D.; Sanchez, C.; Lebeau, B.; Patarin, J. *Chem. Rev.* **2002**, *102*, 4093.
(9) Sayari, A.; Hamoudi, S. *Chem. Mater.* **2001**, *13*, 3151.
(10) Beck, J. S.; Vartuli, J. C.; Roth, W. J.; Leonowicz, M. E.; Kresge, C. T.; Schmitt, K. D.; Chu, C. T.-W.; Olson, D. H.; Sheppard, E. W.; McCullen, S. B.; Higgins, J. B.; Schlenker, J. L. *J. Am. Chem. Soc.* **1992**, *114*, 10834.
(11) Cheng, Y.-R.; Lin, H.-P.; Mou, Ch.-Y. *Phys. Chem. Chem. Phys.* **1999**, *1*, 5051.
(12) Namba, S.; Mochizuki, A.; Kito, M. *Stud. Surf. Sci. Catal.* **1998**, *117*, 257.
(13) Gol'tsov, Y. G.; Smelaya, Z. V.; Matkovskaya, L. A.; Tsyrina V. V.; Il'in, V. G. *Teor. Eksp. Khim.* **1999**, *35*, 109.
(14) Van Der Voort, P.; Mathieu, M.; Mees, F.; Vansant, E. F. *J. Phys. Chem. B* **1998**, *102*, 8847.
(15) Adams, C. J.; Bradley, A. E.; Seddon, K. R. *Aust. J. Chem.* **2001**, *54*, 679.
(16) Yuan, Z.; Zhou, W. *Chem. Phys. Lett.* **2001**, *333*, 427.
(17) Grun, M.; Unger, K. K.; Matsumoto, A.; Tsutsumi, K. Special Publication − Royal Society of Chemistry (1997), 213 (Characterisation of Porous Solids IV), 81.
(18) Liu, Y.; Pinnavaia, T. J. *J. Mater. Chem.* **2002**, *12*, 3179.
(19) Kim, J. M.; Jun, S.; Ryoo, R. *J. Phys. Chem. B* **1999**, 103, 6200.
(20) Ryoo, R.; Kim, J. M. *J. Chem. Soc. Chem. Commun.* **1995**, 711.
(21) Jaroniec, M.; Kruk, M.; Shin, H. J.; Ryoo, R.; Sakamoto, Y.; Terasaki, O. *Micro. Meso. Mater.* **2001**, *48*, 127.
(22) Edler, K. J.; White, J. W. *Chem. Mater.* **1997**, *9*, 1226.
(23) Luechinger, M.; Frunz, L.; Pirngruber, G. D.; Prins, R. *Microporous Mesoporous Mater.* **2003**, *64*, 201.
(24) Landau, M. V.; Varkey, S. P.; Hershkowitz, M.; Regev, O.; Pevzner, S.; Sen, T.; Luz, Z. *Microporous Mesoporous Mater.* **1999**, *33*, 149.
(25) Chen, L.; Horiuchi, T.; More, T.; Maeda, K. *J. Phys. Chem. B* **1999**, *103*, 1216.
(26) Monnier, A.; Schüth, F.; Huo, Q.; Kumar, D.; Margolese, D.; Maxwell, R. S.; Stucky, G. D.; Krishnamurty, M.; Petroff, P.; Firouzi, A.; Janicke, M.; Chmelka, B. F. *Science* **1993**, *261*, 1299.
(27) Huo, Q.; Margolese, D. I.; Ciesla, U.; Feng, P.; Gier, T. E.; Sieger, P.; Leon, R.; Petroff, P. M.; Schüth, F.; Stucky, G. D. *Nature* **1994**, *368*, 317.

10.1021/cm047901h CCC: $30.25
Published on Web 06/10/2005

given of the materials produced using phosphonium headgroups. A recent report on the lyotropic liquid crystal phase behavior of alkyltrimethyl phosphonium surfactants revealed that the phase diagram of cetyltrimethyl phosphonium bromide (CTPB) is very similar to that of cetyltrimethylammonium bromide (CTAB), showing that the effect of the larger headgroup is compensated by the relatively long alkyl tail.[29] Thus, the prospect of preparing MCM-41 with phosphonium based templates is high. The differences of the size of their headgroups and of their effective charges may result in materials with different and improved properties. Furthermore, they contain a sensitive NMR probe in the form of ^{31}P, which can be used to study the formation mechanism of the mesoporous materials and their properties in detail. Here, we describe a MCM-41 mesoporous material, synthesized with CTPB as the structure-directing agent, which has a "temporary" hydrothermal stability that is the result of the presence of P_2O_5 on its surface, produced during calcination.

Experimental Section

Materials Synthesis. The surfactant was prepared according to the synthetic method of Pindzola and Gin.[29] To obtain highly ordered MCM-41 using CTPB, several attempts were made by varying the concentration of tetraethoxysilane (TEOS) or NH_4OH within the following molar ratios: (1−3) (TEOS):0.21 CTPB:3.9 NH_4OH:26 H_2O or 1 TEOS:0.21 CTPB:(2−6) NH_4OH:126 H_2O. The best quality material was obtained using the following mixture 1 TEOS:0.21 CTPB:3.9 NH_4OH:126 H_2O. In a typical preparation, 0.053 g of the surfactant was stirred in 1.5 mL of water until a clear solution was obtained. Then 0.4 mL NH_4OH (25%) was added, followed by 0.15 mL TEOS (98%). The mixture was stirred for 4 h at ambient temperature, after which the solid was recovered by filtration and allowed to dry at room temperature (RT) for 24 h. This material is referred to as RT-MCM-41(CTPB). The hydrothermal material, HY-MCM-41(CTPB), was prepared by transferring the above reaction mixture, after 4 h of stirring at room temperature, to an autoclave that was then placed in an oven at 100 °C for 4 days. After cooling to RT, the solid material was collected and dried as described above. Calcination was performed on HY-MCM-41(CTPB) at 600 °C for 6 h. The resulting material is referred to as CA-MCM-41(CTPB). For comparison, MCM-41 samples were prepared, using the conventional template CTAB in a molar composition of 1 TEOS:0.12 CTAB:2.4 NH_4OH:74 H_2O. RT-, HY-, and CA-MCM-41(CTAB) samples were prepared as described above. While the pH of the starting gels of the two preparations was the same, the surfactant/TEOS ratio was larger for CTPB than for CTAB, 0.21 vs 0.12.

Characterization. Small-angle X-ray (SAX) diffraction profiles were recorded on a SAX diffractometer, equipped with a Franks mirror and a 1D position sensitive detector (homemade), using Cu Kα (1.54 Å) with a Ni filter.[30] Transmission electron micrographs were obtained with a Philips 120 microscope operated at 120 kV. The sample was ground and deposited on a carbon/collodion-coated 300 mesh copper grid that was treated for 30 s by glow discharge. N_2 adsorption measurements were performed at 77 K with a NOVA-2000 instrument (Quantachrome, version 7.11) using conventional BET and BJH methods (both on the adsorption branch). The samples were degassed under vacuum at 300 °C prior to analysis.

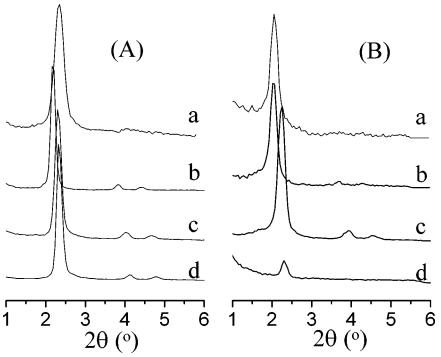

Figure 1. SAX diffraction patterns of (A) (a) RT-MCM-41(CTPB), (b) HY-MCM-41(CTPB), (c) CA-MCM-41(CTPB), and (d) CA-MCM-41(CTPB) after 16 h in water at 100 °C and (B) (a) RT-MCM-41(CTAB), (b) HY-MCM-41(CTAB), (c) CA-MCM-41(CTAB), and (d) CA-MCM-41(CTAB) after 1 h in water at 100 °C.

Solid-state ^{13}C, ^{31}P, and ^{29}Si MAS NMR experiments were carried out on a Bruker DSX 300 spectrometer with a WB 4 mm Bruker MAS probe, at 75.47, 121.49, and 59.6 MHz, respectively. The spinning rate was 5 kHz during the ^{13}C experiments and 10 kHz during the ^{31}P and ^{29}Si experiments. To obtain ^{31}P and ^{29}Si NMR spectra, single Hahn-echo experiments were performed with $\pi/2$ and π pulses of 5 and 10 μs, an echo delay of 100 μs, and repetition delays of 20 and 600 s, respectively. The ^{13}C as well as ^{29}Si spectra were recorded using variable amplitude cross-polarization MAS (VACPMAS) experiments, followed by echo detection. The Hartman−Hahn matching conditions were set around 50 kHz and the duration of the matching times was 5 ms. The echo delays after cross-polarization were 200 and 100 μs and the repetition delays 3 and 5 s for ^{13}C and ^{29}Si, respectively. In all experiments, proton decoupling was employed with an irradiation strength of 80 kHz. The numbers of signal accumulations necessary for obtaining a sufficient signal-to-noise (S/N) value were 128 for ^{31}P and 4096 for ^{13}C and ^{29}Si. The ^{31}P chemical shift scale was referenced to H_3PO_4 (85%) and the ^{29}Si and ^{13}C scales to TMS.

^{31}P NMR measurements on the micellar solution and the reaction mixture were carried out on a high-resolution Bruker Avance DRX 400 spectrometer at 161.97 MHz. A single $\pi/2$ pulse of 6.2 μs and repetition delay of 0.5 s along with ^1H decoupling were applied, and 64 scans were accumulated. The sample spinning rate was 20 Hz.

The samples for the NMR measurements of the reaction mixtures were prepared as follows: a standard liquid NMR tube was filled with 0.63 mL of the micellar solution of CTPB in H_2O (10% D_2O for locking purposes) and NH_4OH with the same molar ratios as used in the synthesis. A sealed capillary with a few drops of H_3PO_4 (85%) was added to the solution as an internal NMR standard. After recording the spectrum of the micelles in the basic solution, 0.05 mL of TEOS was injected to this tube. All the solution NMR experiments were done at a fixed temperature of 293 K.

Results and Discussion

The SAX diffraction patterns of RT-, HY-, and CA-MCM-41(CTPB) are shown in parts a−c of Figure 1A and the values of the *d* spacings are listed in Table 1. The hydrothermal treatment and calcination significantly improved the hexagonal structure. An increase in *d* was observed upon the thermal treatment while the calcination led to a contraction, reducing *d* by 0.7 Å. For comparison, the SAX

(28) Beck, J. S. US Patent 5,057,296, 1991. Degnan, T. F.; Johnson, I. D.; Keville, K. M. Mobil Oil Corp., USA, 1992. Corma Canos, A.; Domine Marcelo, E.; Pena Lopez, M. L.; Rey Garcia, F. Consejo Superior de Investigaciones Cientificas, Universidad Politecnica de Valencia, Spain, PCT Int. Appl., 2000.
(29) Pindzola, B. A.; Gin, D. L. *Langmuir* **2000**, *16*, 6750.
(30) Cheethman, J. J.; Wachtel, E.; Bach, D.; Epand, R. M. *Biochemistry* **1989**, *28*, 8928.

Table 1. *d* Values, in Å, of the Various MCM-41(CTPB) and MCM-41(CTAB) Materials Synthesized[a]

	MCM-41(CTPB)	MCM-41(CTAB)
RT	37.6	40.4
HY	39.1	41.0
CA	38.4	39.1
CA, hydro (1st time)	38.0	destroyed

[a] CA, hydro corresponds to the calcined materials after 16 h in water at 100 °C.

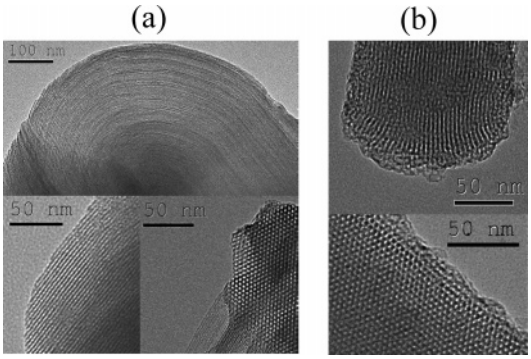

Figure 2. TEM images of (a) CA-MCM-41(CTPB) and (b) CA-MCM-41(CTAB) along different directions.

diffraction pattern of the analogous MCM-41(CTAB) samples are shown in parts a−c of Figure 1B, and their corresponding *d* spacings are listed in Table 1 as well. The general behavior of the two materials is similar, although the MCM-41(CTAB) material is somewhat less ordered as indicated by the width of the d_{100} diffraction. In MCM-41(CTAB), the increase in *d* after the thermal stage is smaller than in MCM-41(CTPB) and the reduction in its *d* value due to calcination is larger (1.9 vs 0.7 Å). These results are similar to those reported earlier for MCM-41(CTAB) in the literature.[21] The transmission electron micrographs (TEM), depicted in Figure 2, confirm the hexagonal structure and the high degree of order. Interestingly, they also show the presence of folded, circular sheets, which were not detected in the CA-MCM(CTAB) sample. Treating CA-MCM(CTPB) in boiling water for 16 h led to a small reduction of the *d* spacing without affecting the long-range order (see part d of Figure 1A). In contrast, CA-MCM(CTAB) lost most of its structure within 1 h as shown in part d of Figure 1B.

Nitrogen adsorption/desorption measurements of CA-MCM-41(CTPB) generated an isotherm typical of mesoporous materials, shown in Figure 3a. It exhibits a slight hysteresis, resulting in a difference between the pore size measured from the desorption branch (25.3 Å) vs the one derived from the adsorption branch (26 Å) (BJH model). This pore diameter is slightly smaller than the 28 Å measured for CA-MCM-41(CTAB) (for the adsorption branch) (see Figure 3b). The BET surface area for CA-MCM-41(CTPB) is 893 vs 972 $m^2\ g^{-1}$ for CA-MCM-41(CTAB). From the *d* values and the pore sizes of the two materials, a wall thickness of 12.7 Å was obtained for CA-MCM-41(CTPB) compared to 11 Å for CA-MCM-41(CTAB).

NMR Measurements. Final Products. The ^{29}Si NMR spectra of HY- and CA-MCM-41(CTPB) and of HY- and CA-MCM-41(CTAB) are shown in Figure 4, and the spectral assignments were made according to the literature.[31,32] The CPMAS spectra are presented in Figure 4a, while the simple

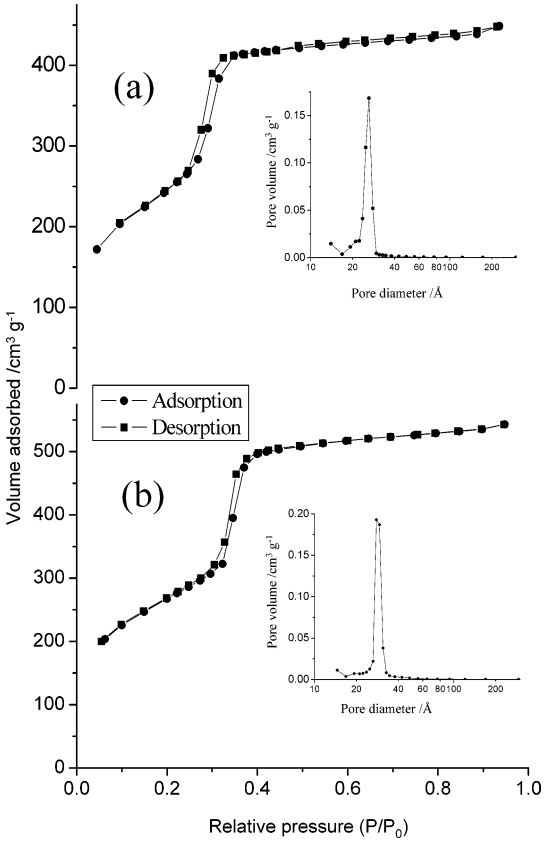

Figure 3. Nitrogen adsorption/desorption isotherms and pore size distribution curves (inset) of (a) CA-MCM-41(CTPB) and (b) CA-MCM-41-(CTAB).

Hahn-echo spectra are shown in Figure 4b. The S/N of the latter is significantly lower than that of the CPMAS spectra because of the relatively small number of signal accumulations recorded (800 vs 4096 during CPMAS) due to a long ^{29}Si T_1 value. These spectra, however, reflect the correct relative intensities of the Q^n signals. In the CPMAS spectra there is a marked reduction of the Q^4 signals of the calcined samples compared to those of the as-synthesized samples. This stems from the removal of the template, which contains many protons, thereby reducing significantly the efficiency of the cross polarization for the Q^4 silica. In the Hahn-echo spectra, the trend is the opposite, as expected. In general, the spectra of the MCM-41(CTPB) and MCM-41(CTAB) materials are very similar, although deconvolution indicates a small, but significant difference between the relative intensities of the Q^n signals, as listed in Table 2. For both as-synthesized and calcined samples, the relative intensity of the Q^4 signal is somewhat higher for MCM-41(CTPB) than for MCM-41(CTAB).

The ^{13}C NMR spectra of the surfactants in HY-MCM-41-(CTPB) and HY-MCM-41(CTAB) are shown in Figure 5a. The spectral assignments are noted in the figure and are comparable with literature values of CTAB[33] and CTPB-related compounds.[34] The spectra of the calcined samples did not show any ^{13}C signals, as expected. Figure 5b shows

(31) Maciel, G. E.; Sindorf, D. W.; Bartuska, V. J. *J. Chromatogr.* **1981**, *205*, 438.
(32) Sindorf, D. W.; Maciel, G. E. *J. Am. Chem. Soc.* **1981**, *103*, 4263.
(33) Lavine, B. K.; Cooper, W. T., III; He, Y.; Hendayana, S.; Han, J. H.; Tetreault, J. *J. Coll. Interface Sci.* **1994**, *165*, 497.

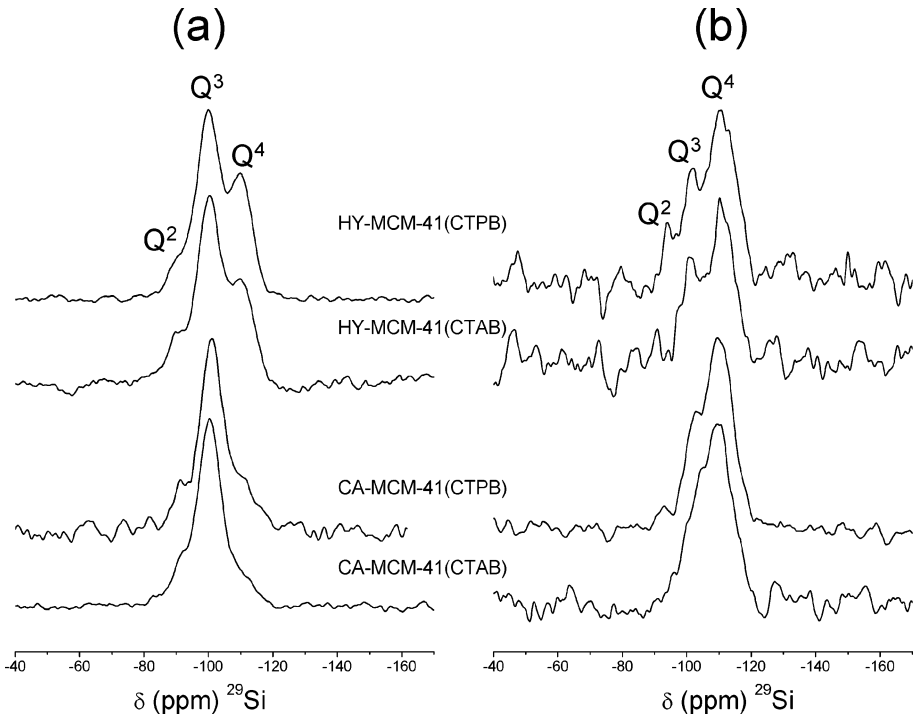

Figure 4. ^{29}Si NMR of MCM-41(CTPB) and MCM-41(CTAB) samples as indicated in the figure. (a) VACPMAS spectra, (b) Hahn-echo MAS spectra.

Table 2. Relative Intensities (%) of the Q^n NMR Signals for Samples of MCM-41(CTPB) and MCM-41(CTAB) Obtained from Hahn-Echo MAS and VACPMAS ^{29}Si NMR[a]

	Hahn-echo (±4%)			VACPM AS (±0.5%)		
	Q^2	Q^3	Q^4	Q^2	Q^3	Q^4
HY-MCM-41(CTAB)	3	29	68	7	64	29
CA-MCM-41(CTAB)		35	65	8	84	8
HY-MCM-41(CTPB)	5	24	71	6	59	35
CA-MCM-41(CTPB)	2	23	75	7	78	15

[a] The experimental error is indicated in parentheses.

the ^{31}P spectra of the MCM-41(CTPB) samples. The spectrum of HY-MCM-41(CTPB) exhibits two overlapping signals at 26.2 and 26.8 ppm, which indicates the presence of two slightly different environments of the phosphonium. Calcination resulted in a significant decrease of the ^{31}P signals along with a considerable shift to 0.7 and 0.1 ppm, close to the chemical shift value of phosphoric acid. These shifted lines are an indication of the presence of inorganic orthophosphate types of species after calcination. The presence of these species, however, did not lead to a significant reduction in the pore volume. Evacuation of the calcined sample for 18 h at room temperature led to a considerable broadening and shift of the signals to 2 and −9 ppm, with no detectable change in their overall intensity (see top spectrum, Figure 5b).

Adding 25 mg of CA-MCM-41(CTPB) to 2.5 mL doubly distilled water yielded a solution with a pH of 2.6, and after boiling this solution for 1 h, the pH decreased further to 2.3. The solid obtained after filtering and drying did not show any detectable ^{31}P signal. Reintroducing this solid into 2.5 mL of water gave a solution with a pH of 6.3. On the basis of these results, we assign the residual phosphorus species to P_2O_5 and attribute the change in the chemical shift induced by the evacuation of the calcined sample to changes in its hydration state. This P_2O_5 is easily removed by washing, without deteriorating the structure, as was shown by the SAX results.

The presence of the residual P_2O_5 in the calcined material explains the hydrothermal stability observed for CA-MCM-41(CTPB) as compared to CA-MCM-41(CTAB). Once suspended in water, the P_2O_5 leaches into the solution and makes it acidic, i.e., the acidity was generated in situ. Boiling CA-MCM-41 in a pH ∼2 solution, which is close to the isoelectric point of silica,[35] where the dissolution rate is the lowest, does not destroy the structure. This was tested by placing CA-MCM-41(CTAB) for 1 h in a boiling solution at pH 2, after which the material was still structured. Once the P_2O_5 is removed from the pores of CA-MCM-41-(CTPB) it is no longer hydrothermally stable and boiling it in water for 1 h led to a significant deterioration of the structure.

Hence, the major difference between the MCM-41 materials prepared with CTPB and CTAB is the "temporary" hydrothermal stability of MCM-41(CTPB). Although not permanent, this has some advantage because it provides a long shelf life of the calcined material, as long as the residual P_2O_5 is not removed. Indeed, we found that there was no change in the SAX pattern of MCM-41(CTPB) 10 months after calcination, while MCM-41(CTAB) completely lost its structure. After the removal of P_2O_5 the material becomes as susceptible as its CTAB counterpart.

Reaction Mixture. In addition to the ^{31}P nucleus being an excellent probe for the characterization of the as-synthesized and calcined MCM-41(CTPB) it can be used during in situ studies, focusing on the organic−inorganic

(34) Riddell, F. G.; Rogerson, M.; Turnbull, W. B.; Fülöp, F. *J. Chem. Soc., Perkin Trans.* **1997**, *2*, 95.

(35) Brinker, C. J.; Scherer, G. W. *Sol−gel science: the physics and chemistry of sol−gel processing*; Academic Press: New York, 1990; pp. 103−107.

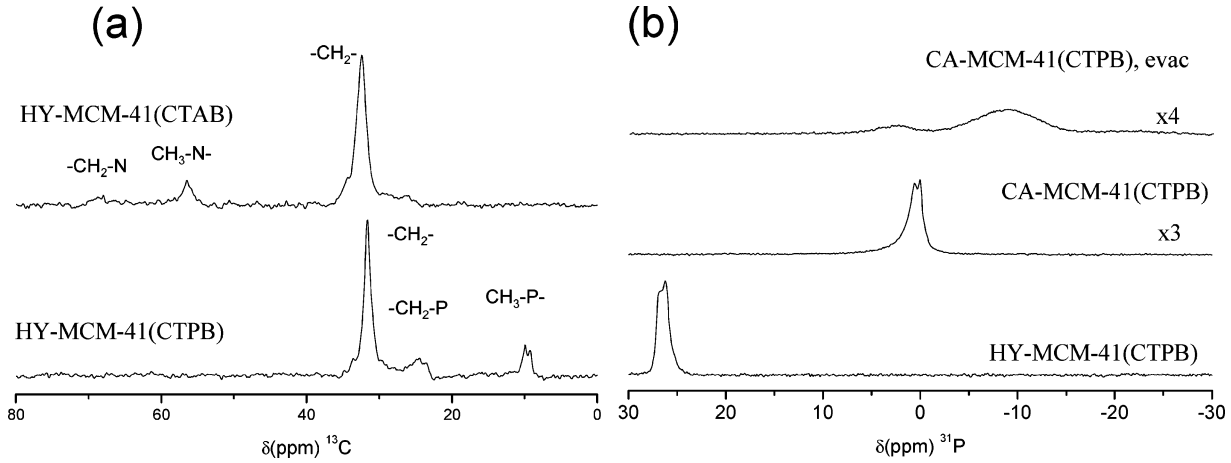

Figure 5. (a) ^{13}C VACPMAS NMR spectra of HY-MCM-41(CTPB) and HY-MCM-41(CTAB); (b) ^{31}P Hahn-echo MAS NMR spectra of MCM-41(CTPB) samples as noted on the figure.

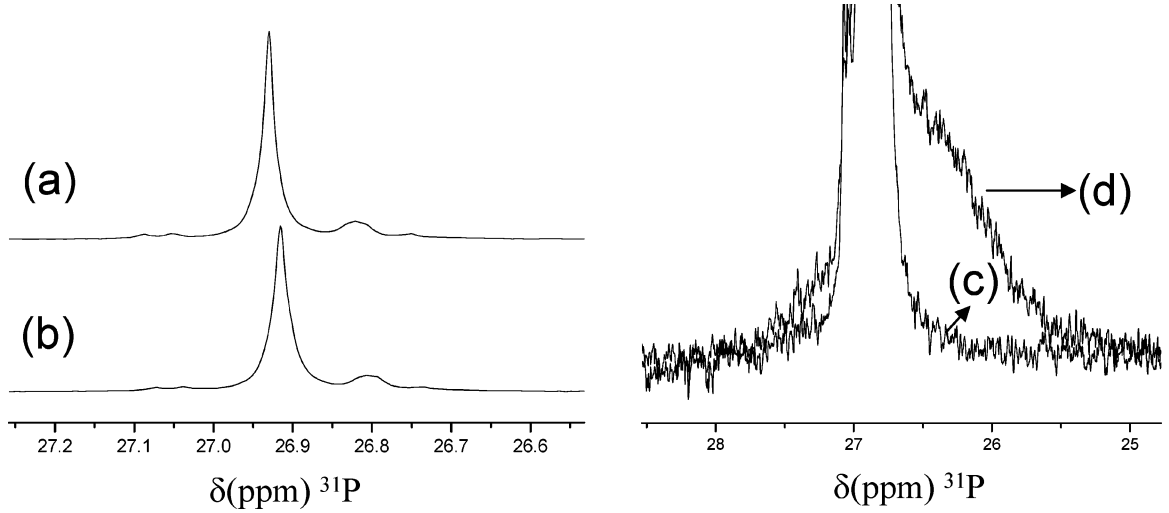

Figure 6. High-resolution ^{31}P NMR spectra of (a) micellar solution of CTPB, (b) same as (a) 12 min after the addtion of TEOS, (c) magnification of (b), and (d) same as (a) 1 h after the addition of TEOS.

interface, at which it is located. Its high natural abundance and high gyromagnetic ratio eliminate the problem of sensitivity encountered with ^{14}N and ^{29}Si, thus allowing a rapid acquisition of its spectrum, which is essential for time-resolved studies. Furthermore, its wide range of chemical shifts and its high sensitivity to subtle changes in its environment along with its special location make it a better NMR probe than the protons. Figure 6 shows spectra acquired at different stages of the reaction, demonstrating the potential of such studies. The spectrum of the micellar solution, prior to the addition of TEOS, yields a signal at 26.93 ppm which shifts 2.2 Hz downfield 12 min after the addition of TEOS (Figure 6a). After 1.5 h of reaction a broad asymmetric signal, spanning ~1 ppm is visible after magnification of the spectra. This signal is absent in the 12-min spectrum, as can be seen from Figure 6b. Interestingly, the sharp signal persists, along with the broad one, for at least 24 h, after the reaction has been completed. We tentatively assign the broad signal to suspended mesostructured hexagonal material and the sharp signal to CTPB molecules either in the solvent or in micelles that remained in the clear liquid after precipitation, however, further measurements will have to be performed to obtain an unambiguous assignment. The acquisition time of all traces in Figure 6 was 160 s, but if only the line position of the sharp signal is of interest, the acquisition time can easily be reduced to 11 s. Hence, using a fast mixing apparatus will allow monitoring the reaction development at very early stages with a relatively high time resolution.

Conclusion

Highly ordered MCM-41 with a "temporary" hydrothermal stability has been synthesized using a phosphonium-based surfactant. The calcined material contains residual P_2O_5 that is produced by the decomposition and oxidation of the surfactant. This residue has almost no effect on the pore volume but protects the material against hydrolysis, thus lending it a long shelf life. The P_2O_5 can easily be removed by washing after which the material becomes susceptible to hydrolysis under neutral and basic conditions, just like any MCM-41 sample that did not undergo special treatment to increase its hydrothermal stability.

Acknowledgment. The authors thank Dr. Ronit Popovitz-Biro for acquiring the TEM images. This research was supported by the center of excellence "Origin of ordering and functionality in mesostructured hybrid materials" supported by The Israel Science Foundation (Grant No. 800301-1).

CM047901H